Magnetic Confinement Theory Summary

TH Contributions = 191

Transport & Confinement > 40% Gyro kinetics, turbulence, heat, particle and momentum transport

Edge Pedestal ~ 20% **--** ELMs, 3D effects

SOL & Divertor – heat flux on targets, 3D, coupling to core, plasma-wall interaction

MHD stability & Disruptions – emphasize on Runaway Electrons

Energetic Particle physics – AEs, EPMs, associated transport

Integrated Modeling

Transport and Confinement

TH/P3-2: **Characteristics of turbulent transport in flux-driven toroidal plasmas**

Y. Kishimoto, K. Imadera, H. Liu, W. Wang, K. Obrejan, J.Q. Li., Kyoto University

We have presented an overall picture of ITG driven turbulent transport, a long-standing problem over 30 years, by achieving global flux-driven gyro-kinetic toroidal system sustained by heat source and sink incorporated with generation of global mean radial electric field.

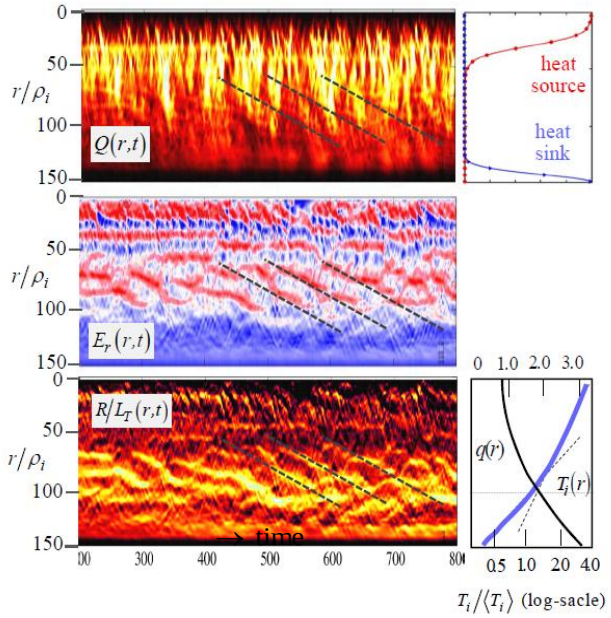

Temporal evolution of heat flux, radial electric, and scale-length

	4 types of transport event (3 non-diffusive)	Correlation length
①	Neo-classical transport and diffusive part of turbulent transport	$\ell_c \sim \rho_i$
②	Radially Localized avalanches with fast time scale toward both core and edge	$\ell_c \sim \rho_i - \sqrt{L_T \rho_i}$
③	Radially extended global ballooning type modes with meso- to macro scale causing instantaneous and intermittent bursts	$\ell_c \sim \sqrt{L_T \rho_i} - L_T$
④	Radially localized avalanches with slow time scale coupled with the evolution of ExB shear layer and pressure corrugation	$\ell_c \sim \sqrt{L_T \rho_i} - L_T$

Characteristics of transport

- Resilience and stiffness in profile weakly depending on heating
- Self-similarity in relaxation keeping specific function form and SOC type intermittent bursts.

③ Origin of global bursts and stiffness

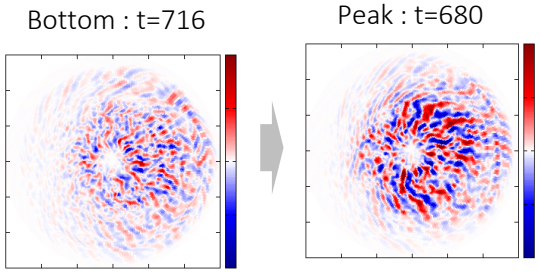

Instantaneous phase alignment of smal eddies leading to extended structure

Size scaling of heat flux eddies

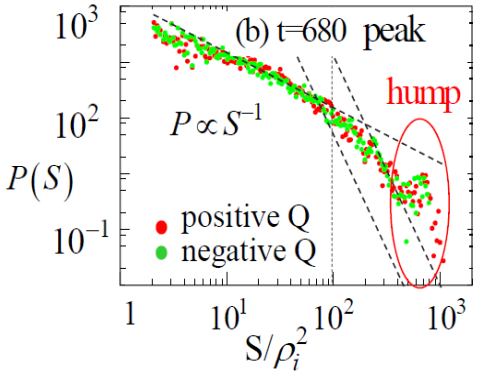

Hysteresis and Fast Timescale in Transport Relation of Toroidal Plasmas

OV/P-8

by K. Itoh, et al.

1. In addition to bifurcation in Improved Confinement, transport hysteresis in core plasmas is widely observed. (LHD, DIII-D, and is highly plausible in TJ-II, KSTAR,….)

LHD, Inagaki et al.

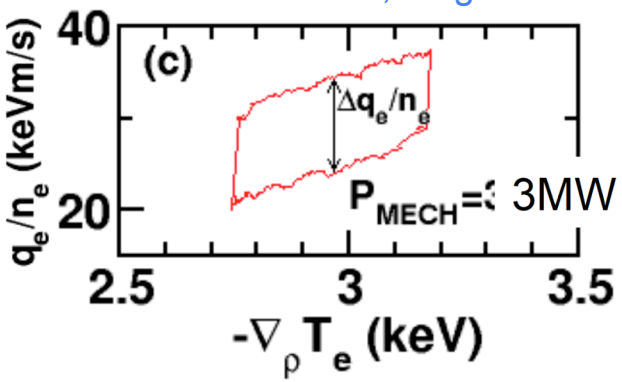

2. The core hysteresis involves two elements:
   1. Direct influence of heating on transport/fluctuations
   2. Interaction at long distance

3. A theory is developed to explain that '*The heating heats turbulence*'. It is attributed to a possible origin of hydrogen isotope effect on confinement time.

Enhancement by heating — Driven by gradients

$$\langle \varphi_1 \varphi_1 \rangle = \frac{1}{1 - \gamma_h \chi_0^{-1} k_\perp^{-2}} \langle \varphi_1 \varphi_1 \rangle_0$$

$$\gamma_h = \frac{\delta P_{heat}}{\delta p}$$

S. I. Itoh, et al. Nucl. Fus. **57** (2017) 022003

4. This hysteresis has the impact on the 'time scale' (at transition and back-transition) in the control system of fusion devices.

TH/P2-27: A New Understanding of the Bootstrap Current in Steep Edge Pedestal

R. Hager, C. S. Chang

- The bootstrap current in the H-mode pedestal has been studied with the global, gyrokinetic-neoclassical code XGCa.
- Contrary to conventional neoclassical theory, the trapped particle contribution to the bootstrap current can be significant in realistic tokamak geometry, especially in spherical tokamaks.
- A new bootstrap current formula valid for the H-mode pedestal has been developed based on numerous XGCa simulations in different realistic, diverted tokamak equilibria. It includes corrections for large trapped particle fraction and finite orbit-width effects.

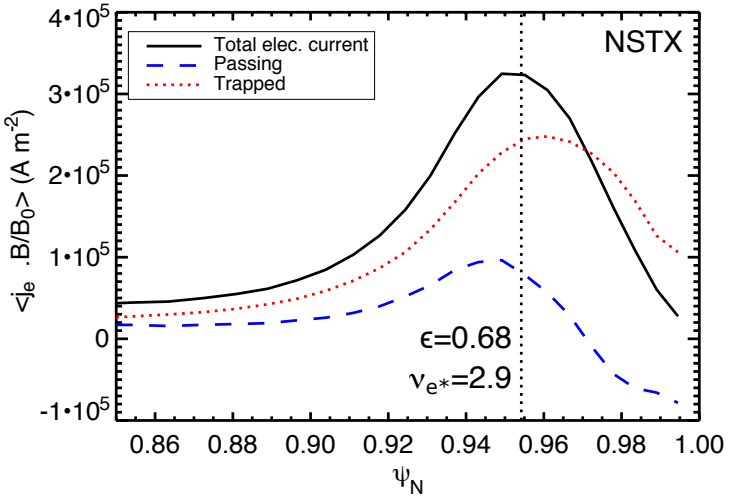

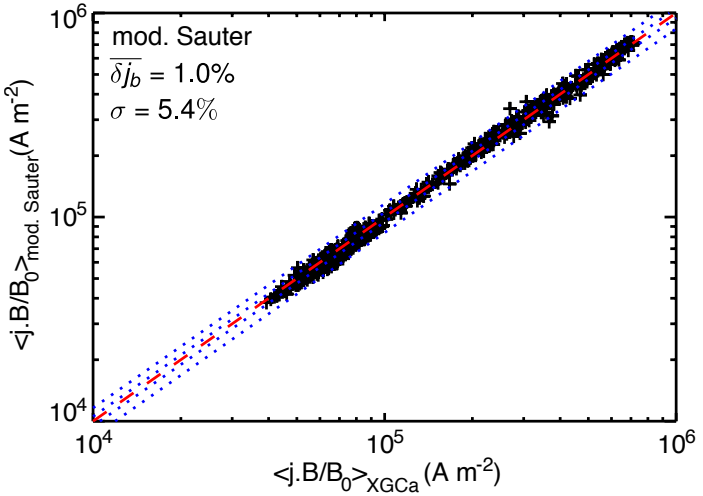

TH/P3-21: Nonlocal Plasma Response to Edge Perturbation in Tokamak

by M. Yagi *et al*

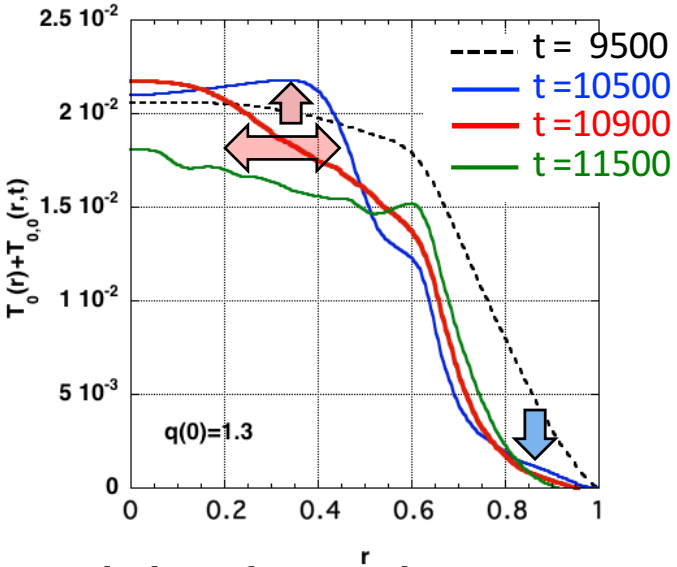

Time evolution of mean electron temperature (in poloidal Alfven time unit).

Nonlocal response of electron temperature fluctuation is investigated using 5-field RMHD model.

Density source and cooling sink are introduced into density and electron temperature evolution equations, respectively.

After density source and cooling sink are turned on near the edge (t = 9500) ⇩, the mean electron temperature increases at the central region ⇧.

The profile relaxation occurs after density source and cooling sink are turned off (t = 10500). Meso-scale mode (*streamer*) plays a role for profile relaxation (t = 10900) ⇔.

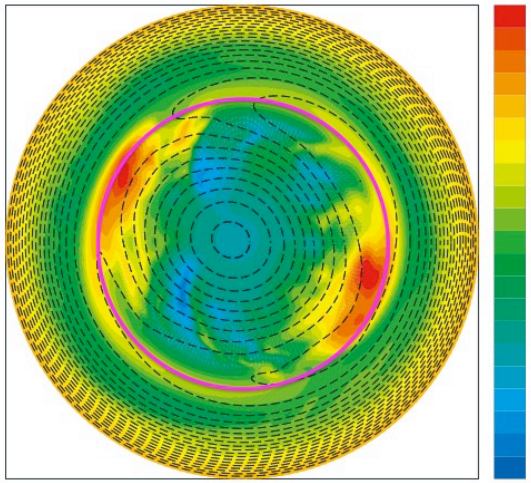

Contour Plot of Fluctuating Electron Temperature at t = 10900.

ρ* Scaling of Intrinsic Drive Projects to a Torque Comparable to that from Neutral Beams on ITER

- **Experimental scaling determined in joint study with JET**
  - Favorable scaling still leads to relatively low level of rotation

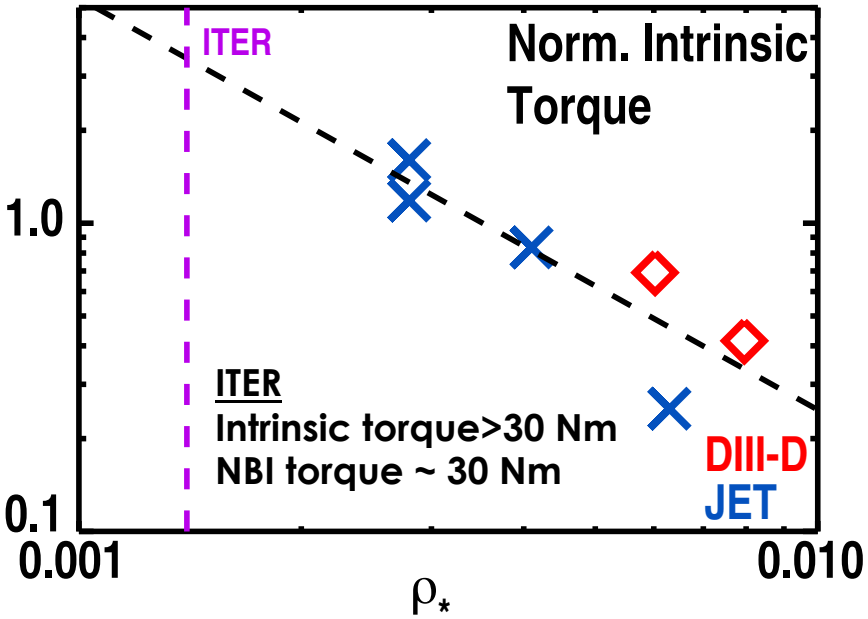

- **Simulations with GTS gyro-kinetic code reproduces reversal of core intrinsic rotation**

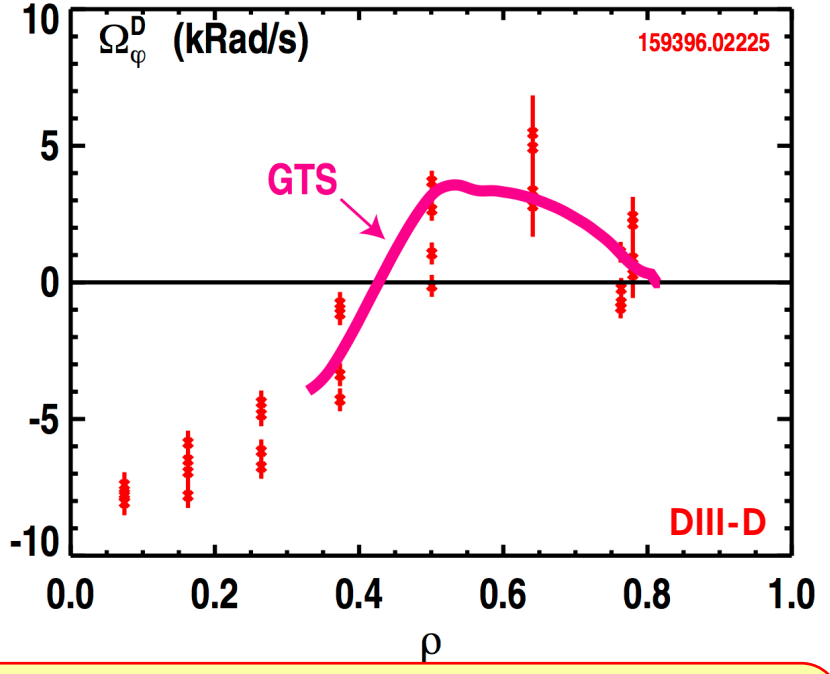

Grierson – EX/11-1
Wang - TH-C/P3-12
deGrassie – EX/P3-13

Although intrinsic rotation projected to be low, profile effects may still lead to improved performance

TH/P3-1 Full-f gyrokinetic simulation including kinetic electrons

Y. Idomura (JAEA), Y. Asahi (JAEA), N. Hayashi (QST), H. Urano(QST)

ECRH modulation tokamak experiments observe rotation changes without torque input

- Important for rotation control in ITER
- Fast profile changes in ~10ms
- Momentum transport is largely unknown

Electron heating modulation numerical experiments using full-f gyrokinetic code GT5D

- New kinetic electron model [Idomura,JCP16]
- Full-f ITG-TEM simulation over ~20msec
- Ion heating is switched to electron heating

Validation against ASDEX-U [McDermott,PPCF11]

- Transition from ITG (ω<0) to TEM (ω>0)
- Density peaking in TEM phase
- Rotation change in ctr-current direction

→Toroidal angular momentum balance shows rotation drive induced by particle transport

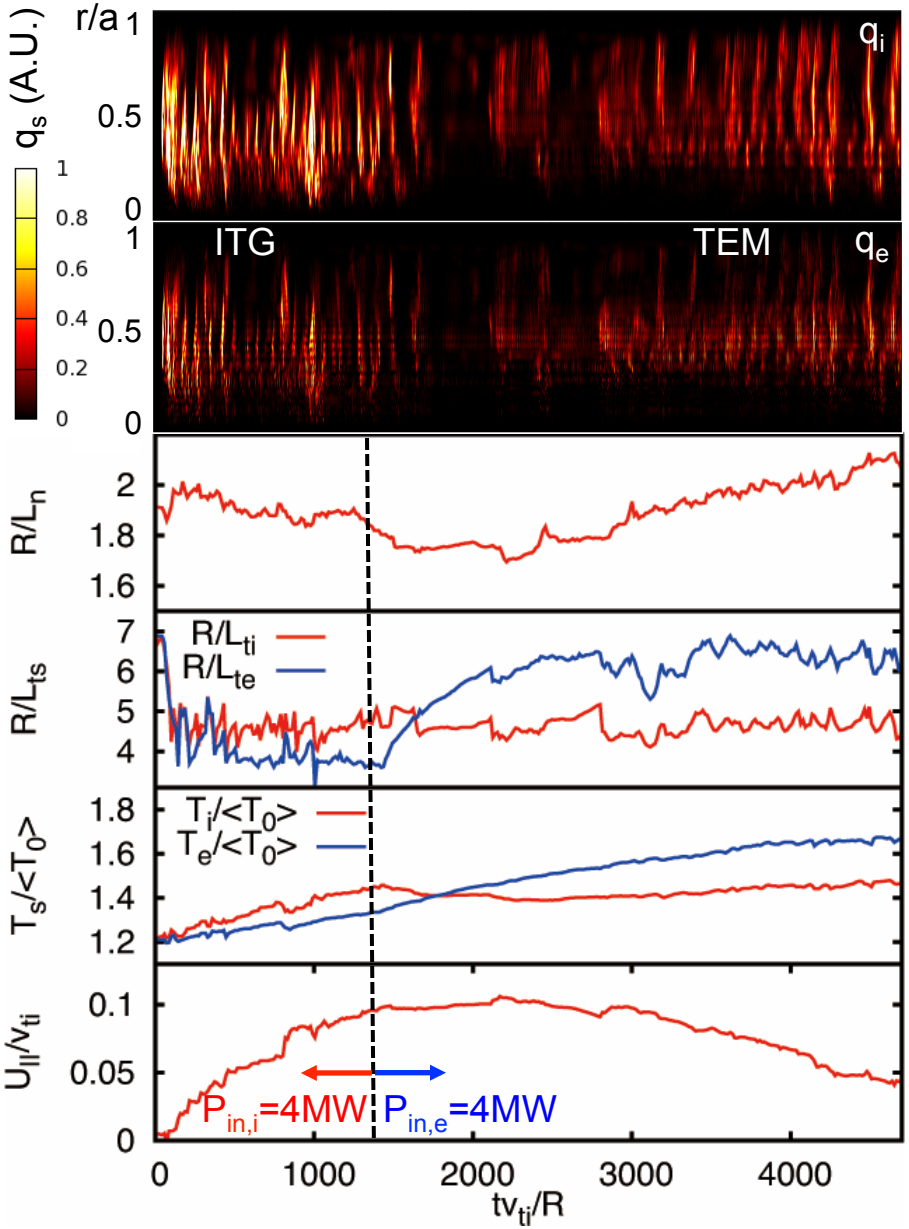

Physics behind role of electron heating in avoiding W accumulation is further clarified

- Electron heating increases W turbulent diffusion to offset neoclassical convection
- Nonlinear GK simulations find W diffusion is maximum when Qe ≈ 1.5 Qi
- In AUG, W peaking factor decreases with increasing electron heating fraction
- At high ECH power, hollow core W densities in the presence of MHD (1,1) modes
- Combined JET and AUG analysis leads to the expectation that neoclassical transport is reduced in a reactor plasma

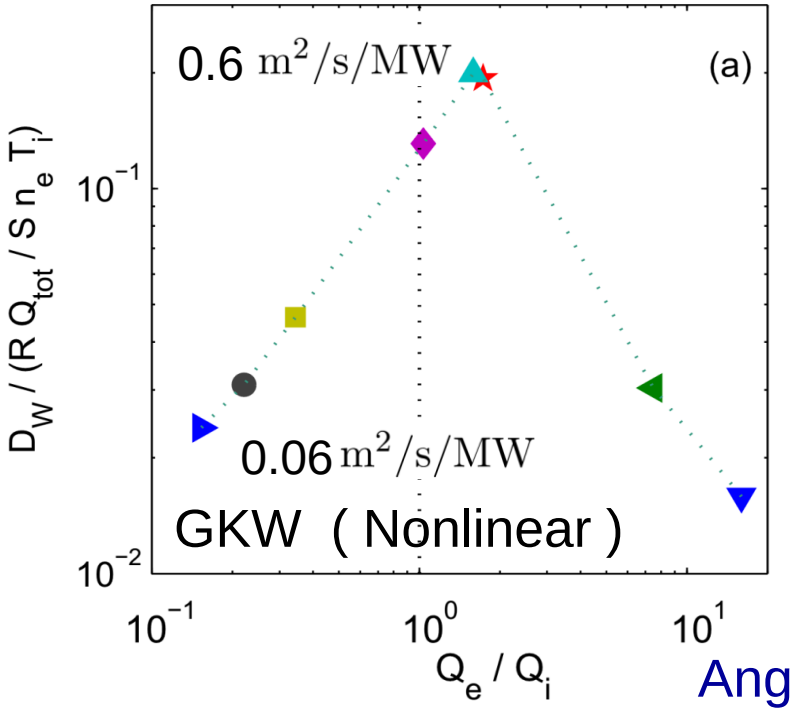

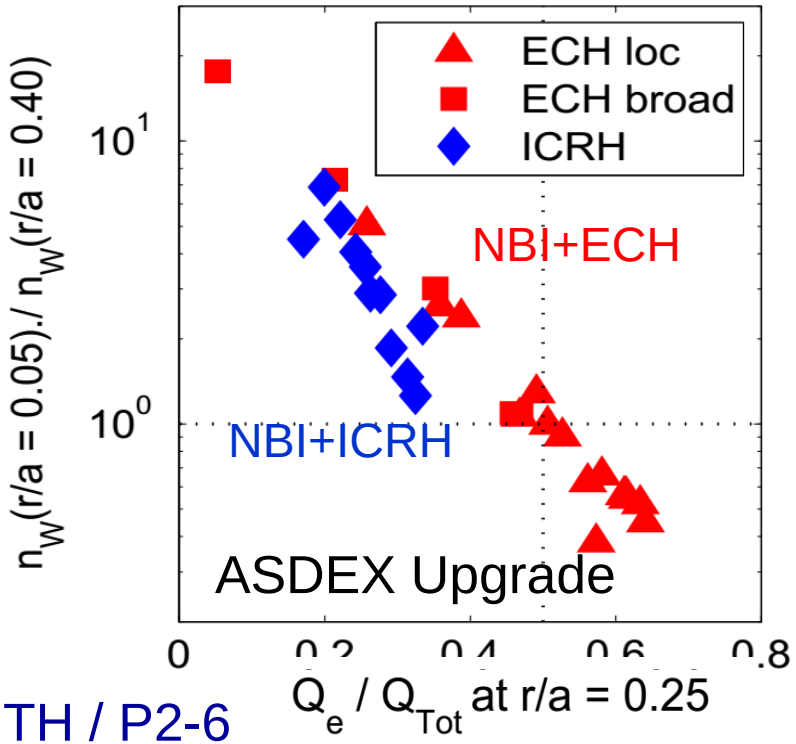

Angioni et al TH / P2-6

Synergetic effects of neoclassical and turbulent processes on impurity transport

- Turbulent Reynolds stress drives flow poloidal convective cells

→ poloidal asymmetries of the impurity density → change neoclassical impurity flux

X. Garbet TH/3-1

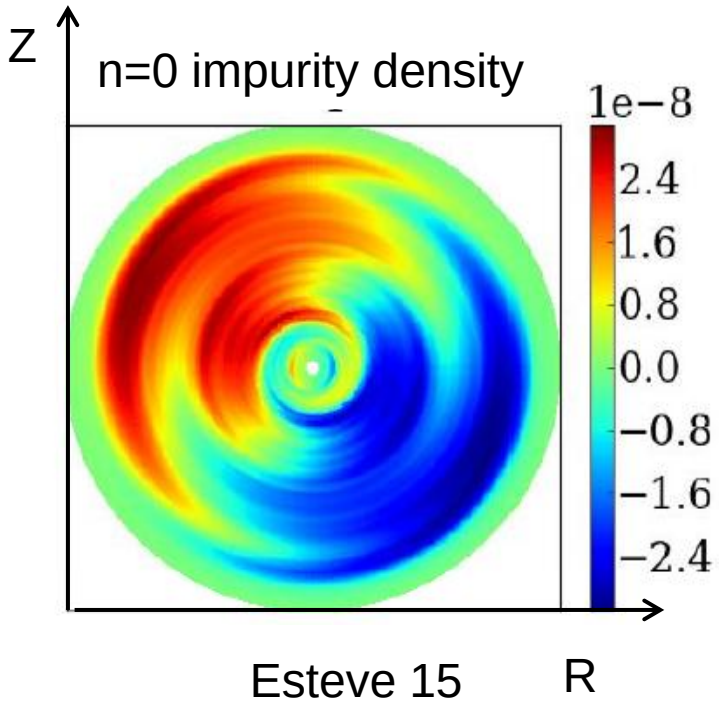

Esteve 15

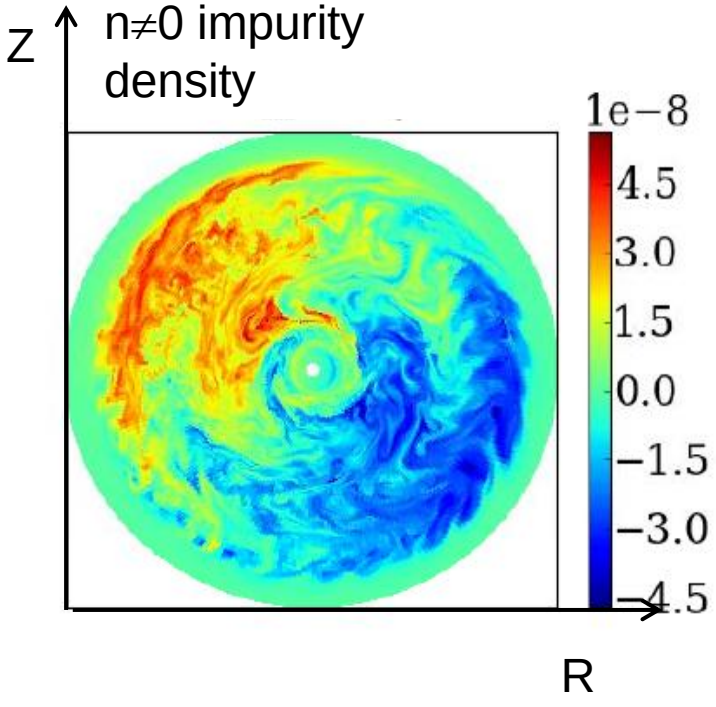

Edge & Pedestal

Non-linear MHD modelling of Edge Localized Modes dynamics.

M. Becoulet (France), M. Kim, G. Yun (Korea) et al. TH/P1-24

The non-linear MHD modelling of full ELM dynamics using JOREK code including toroidal rotation and two fluid diamagnetic effects for KSTAR pulse reproduced many ECEI diagnostic observations.

Density filaments in ELM crash.

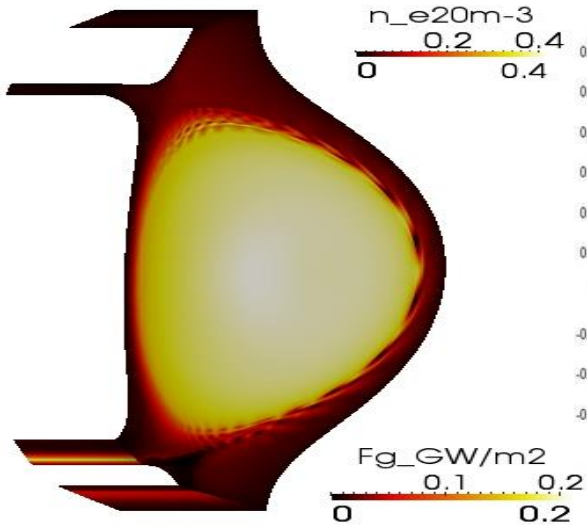

Poloidal rotation (V~5km/s) of δTe (N=8) before ELM crash.

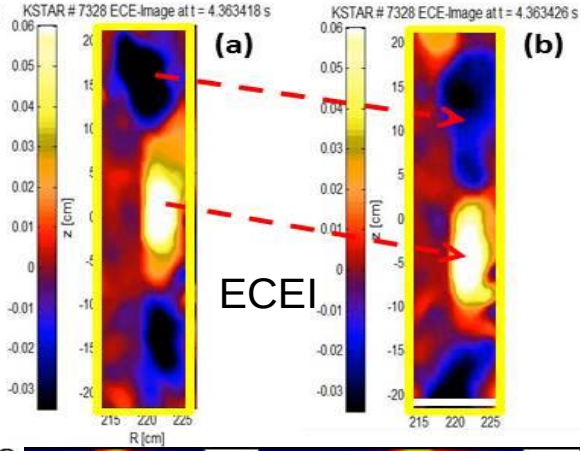

δTe spectra in multi-harmonic multi-cycles modelling in inter-ELM phase are similar to experimental (ECEI).

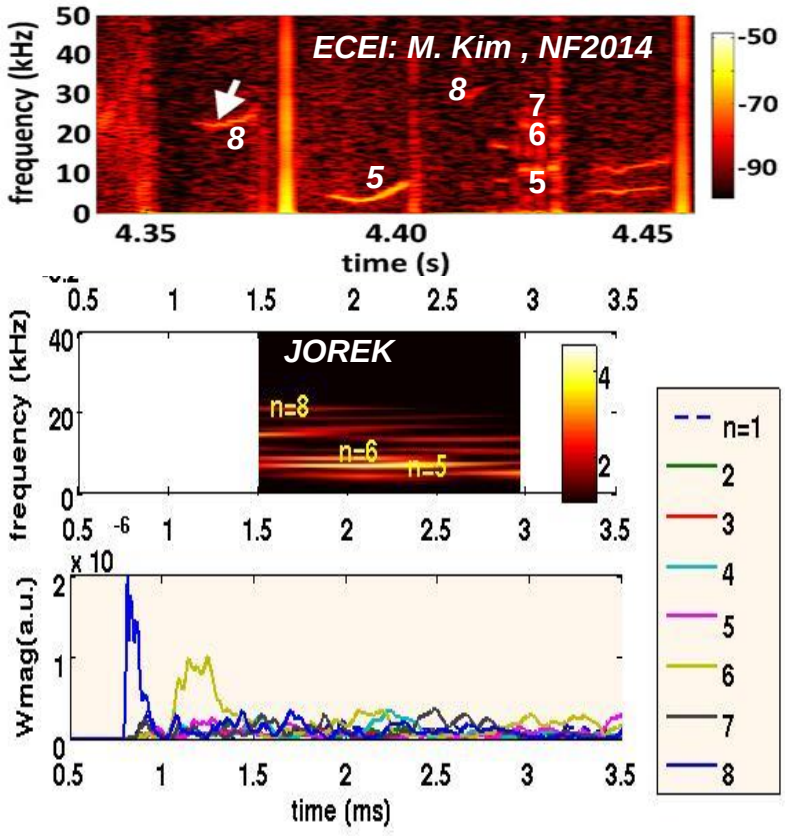

Edge ergodisation during ELM.

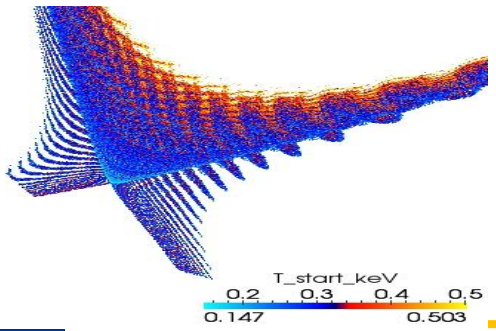

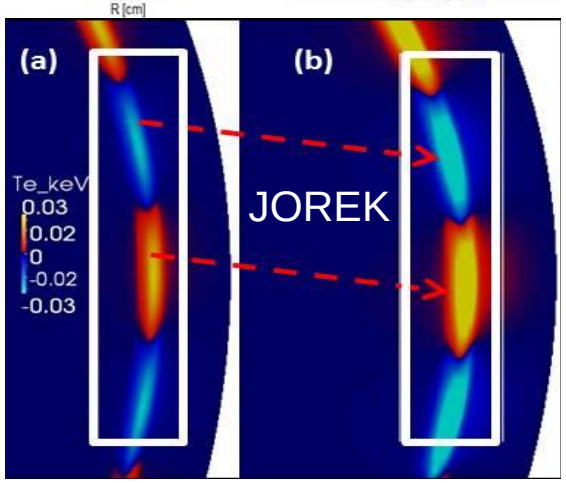

TH/8-1 N. Aiba et al.
Diamagnetic MHD equations for plasmas with fast flow and its application to ELM analysis in JT-60U and JET-ILW

- Diamagnetic MHD equations and the corresponding linearized equation were derived by introducing an ordering between MHD and drift orderings.
- These equations realize to analyze MHD stability with the ion diamagnetic drift (ω_{*i}) effect in rotating tokamak plasmas.
- By solving the linearized equation with the MINERVA-DI code, it was found that plasma rotation can destabilize peeling-ballooning modes due to minimizing the ω_{*i} effect.
- This destabilizing effect has large impact on the type-I ELM stability in JT-60U and JET with ITER like wall (ILW).

Comparison of ELM stability boundary in static (blue) and rotating (red) cases in JT-60U and JET-ILW.

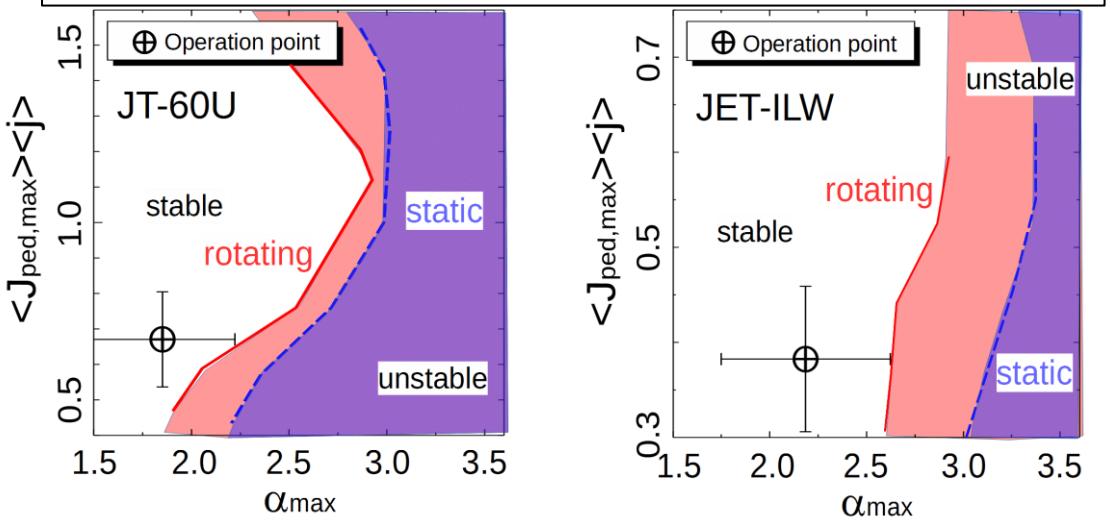

Sol & Divertor

3D Edge Transport Modeling Shows Linear MHD Solutions Do Not Simultaneously Match Pedestal and Divertor Conditions

- **Plasma response required to support measured pedestal gradient ➔**
  - Vacuum fields show too much stochasticity
  - Ideal MHD solution matches core gradient, but flattened near separatrix
- **Strong screening in extended MHD solutions removes downstream lobes and T_e peaking**
  - Results sensitive to edge rotation

✓ **No B-field model tested can explain pedestal and divertor data simultaneously**

EMC3-EIRENE Energy Equation Solutions

Upstream

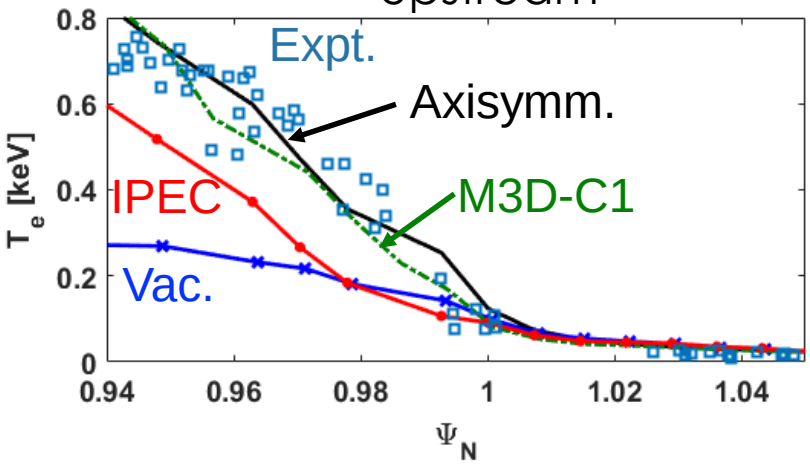

Downstream

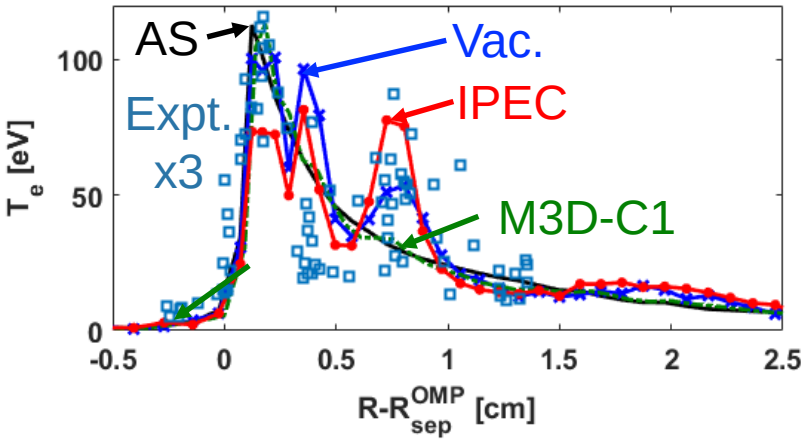

Edge and divertor plasma: detachment, stability, and plasma-wall interactions

S. I. Krasheninnikov[1]†, A. S. Kukushkin[2,3], Wonjae Lee[1], A. A. Phsenov[2,3], R. D. Smirnov[1], A. I. Smolyakov[4], A. A. Stepanenko[3], and Yanzeng Zhang[1]

[1]University of California San Diego, La Jolla, CA 92093, USA; [2]Kurchatov Institute, Kurchatov sq. 1, 123182 Moscow, Russia; [3]NRNU MEPhI, Kashirskoje av. 31, 115409 Moscow, Russia; [4]University of Saskatchewan, 116 Science Place, Saskatoon, SK S7N 5E2, Canada

Physics of divertor detachment

The results of thorough 2D simulation of edge plasma with SOLPS code (Krasheninnikov et al., PoP, 2016) confirm theoretical predictions that impurity radiation loss and plasma recombination are the main reasons of the rollover of plasma flux to divertor targets in the course of divertor plasma detachment (Krasheninnikov, CPP, 1996; PoP, 1997). Although ion-neutral interactions are important for maintaining appropriate upstream and divertor plasma parameters, they are not responsible *per se* for the reduction of plasma flux to the targets (see Fig. 1).

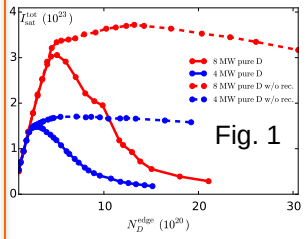

Fig. 1

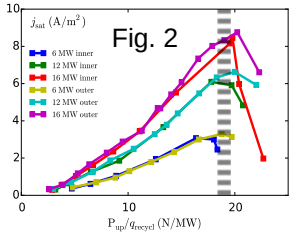

Fig. 2

2D simulations also confirm that the condition governing an onset of the rollover of plasma flux to the target at some particular flux tube can be written as $P_{up}/q_{recycl} \tilde{>} (P_{up}/q_{recycl})_{crit}$ where P_{up} and q_{recycl} are the upstream plasma pressure and the heat flux to recycling region (Krasheninnikov, et al., JNM, 1999) (see Fig. 2). Impurity driven local thermal instabilities in ITER-like plasma can cause significant (~50%) variation of the heat load on divertor target (Fig. 3) Smirnov, et al., PoP, 2016

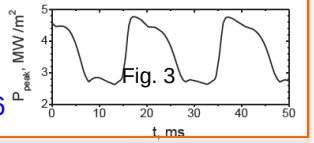
Fig. 3

Generation of blobs and dynamics of drift waves

Blobs play a crucial role in the Scrape-Off-Layer plasma transport. However, there is compelling experimental evidence that high density plasma blobs exist already inside separatrix where they are moving predominantly in poloidal direction. In (Krasheninnikov, PLA, 2016) it was shown that by retaining a non-linear Boltzmann factor in Hasegawa-Mima equation

$$de^{\phi}/dt - \rho_s^2 \nabla \cdot (e^{\phi} d\nabla\phi/dt) + V_{DW} e^{\phi} \vec{e}_x \cdot (\nabla\phi \times \vec{b}) = 0$$

one can find solution of a large amplitude $n/n_0 \sim 3$ virtually solitary drift waves moving in poloidal direction. Numerical simulations show that such large bursts of density can emerge even from initial perturbations of small amplitude (Zhang & Krasheninnikov, submitted).

Current-conv. Inst. in detached plasmas

In (Krasheninnikov & Smolyakov, PoP, 2016) it was shown that Current-Convective Instability (CCI), which for a tokamak condition is usually stabilized by high parallel electron heat conduction can develop in cold detached plasmas for the conditions where inner divertor is detached while outer is still attached. For this case asymmetry of plasma temperatures near the targets causes a large drop of electrostatic potential within cold inner divertor, which drives electric current and CCI. Once outer divertor detaches CCI is no more. These findings can explain the AUG data on radiation fluctuations from inner divertor (Potzel, et al., NF, 2014).

Formation of the layer of Helium nano-bubbles in Tungsten

Due to its low solubility He tends to precipitate into bubbles when embedded into metals. For a sample temperature below 1000 K, the layer of He nano-bubbles of the thickness ~30-50 nm and diameter ~ 2 nm was observed experimentally in the near-surface region of He irradiated tungsten, for He energies below the sputtering threshold and fluxes relevant to the ITER conditions (e.g. Kajita, et al., NF, 2009). This layer saturates at He fluence ~3×10^{20} cm^{-2} regardless the magnitude of He flux. However, the MD simulations of the formation of He nano-bubbles accounting only for self-trapping of He atoms were unable to fit these experimental observations. In (Krasheninnikov & Smirnov, NF, 2015) it was shown that each growing He nano-bubble produces dislocations in W lattice, which can effectively trap He atoms and can work as the seeds of new nano-bubbles. In Fig. 4 one can see MD simulation results for He clusters formed due to trapping in these dislocations and due to He self-trapping. The reaction-diffusion model describing dynamics of free He and He clusters, which takes into account the generation of traps associated with growing nano-bubbles, allowed to match most crucial experimental data (critical He fluence, thickness of the layer, and bubble diameter).

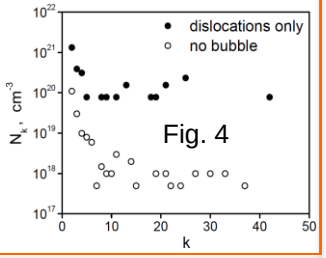

Fig. 4

Divertor heat flux simulations in ELMy H-mode discharges of EAST and other tokamaks

T. Y. Xia[1,2], B. Chen[3,2], T.F. Tang[4,2], B. Gui[1,2], X.T. Xiao[1,2], X. Q. Xu[2], D. H. Li[1], Z. Zheng[1] and EAST Team[1]

[1]ASIPP, [2]LLNL, [3]USTC, [4]DUT

- Six-field two-fluid model in BOUT++ framework is used for the heat flux simulations:
  - Self-consistent turbulent transport
  - Flux limited thermal conduction
  - Neoclassic transport as diffusion terms
  - Sheath boundary conditions on targets
- Validations with DIII-D ELMy H-mode #144382: similar time evolution, narrower width, twice amplitude.

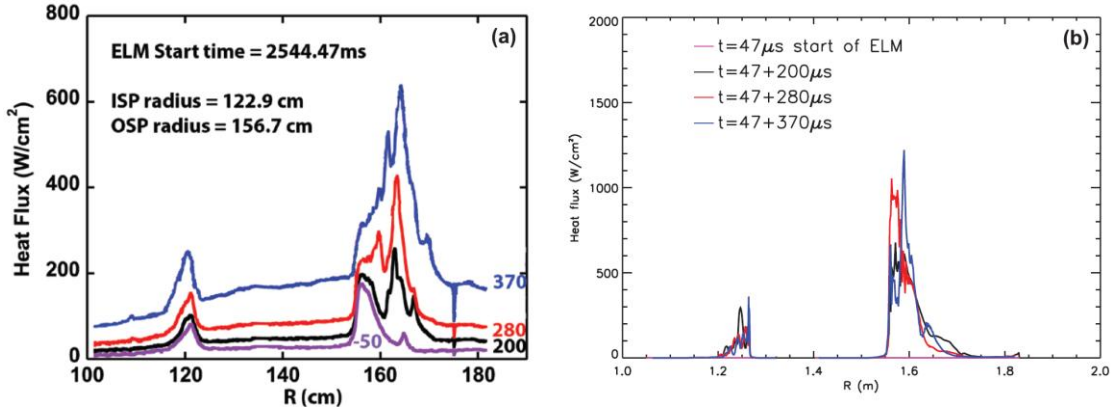

Left: heat flux profiles on targets during ELM burst on DIII-D. Right: Simulated heat flux profiles [1].

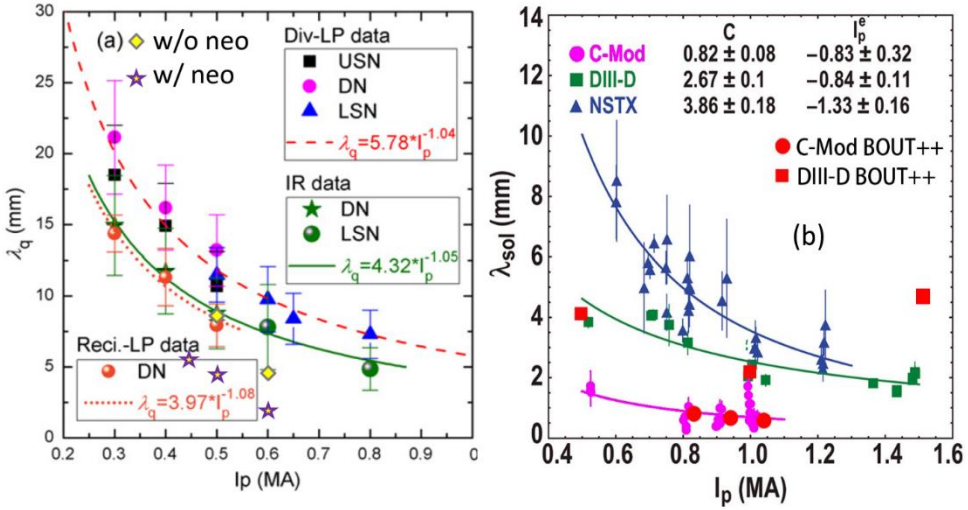

(a) The comparison between simulated SOL width λ_q with EAST experimental statistics. The simulated λ_q shows the similar trends to Ip, but the amplitude is more than half smaller than the measurements. (b) The simulated SOL width compared with multi-machine results.

- H-mode discharges on EAST, DIII-D and C-Mod with different Ip for the SOL width λ_q scaling simulations.
  - Similar trend of λ_q to I_p.
  - Half of the experimental amplitude on EAST: no RF heating effects on edge topology.
  - Good agreement with multi-machine scaling [3] in the range of $0.45MA<I_p<1MA$.
  - Neoclassic transport is important for the low I_p case.

[1] T.Y. Xia and X.Q. Xu, Nucl. Fusion 55, (2013) 113030.
[2] L. Wang, H.Y. Guo, G.S. Xu et al., Nucl. Fusion 54 (2014) 114002.
[3] M.A. Makowski et al, Phys. Plasmas 19 (2012) 056122.

MHD stability, Disruptions, REs

First Principle Fluid Modelling of Neoclassical Tearing Modes and of their Control

Drift-neoclassical model and insights on NTM drive

- Self-consistent fluid drift-neoclassical model implemented in the nonlinear MHD code XTOR
- Bootstrap and pressure perturbations not fully correlated [measure: $R_{bs}(p)$]
- Triggering of a (3,2) NTM obtained by increasing this correlation

~island width

Correlation bootstrap & pressure

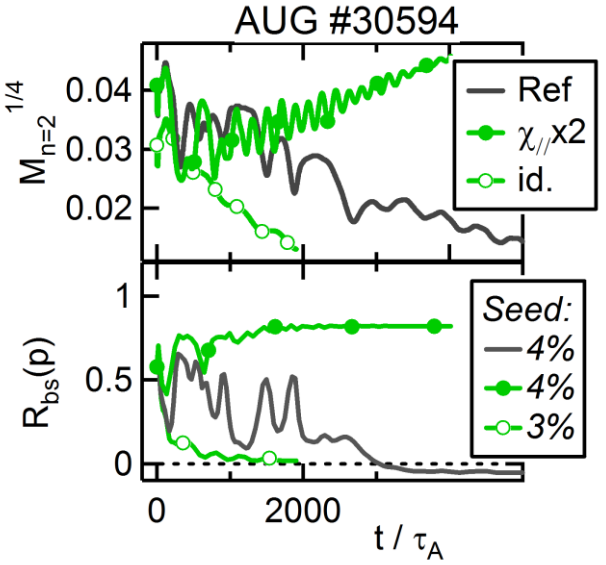

Strategies for island control

- RF current source & controller implemented in XTOR
- Radial sweeping mitigates misalignment risk for preemption and stabilization (TCV&AUG exp.)
- Modulation lowers final size for a broad RF current source
- Alternate modulation allowing nearly continuous O-point hitting (FADIS) reduces stabilization time

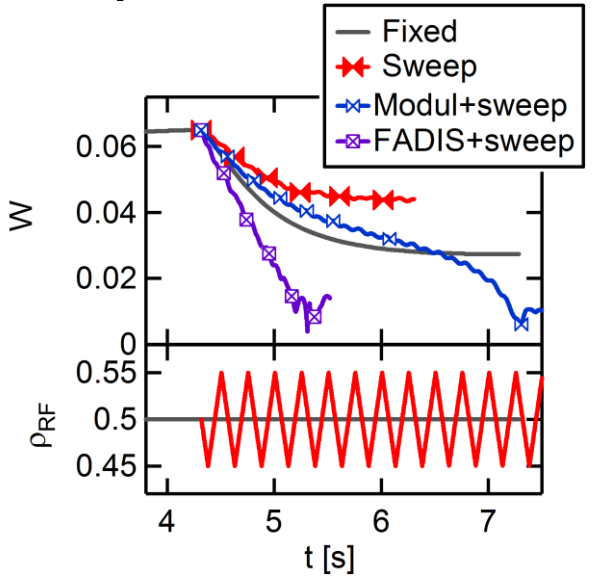

patrick.maget@cea.fr

Toroidal gyrokinetic simulations of the tearing mode

- Toroidal kinetic effects change qualitatively the dynamics of tearing modes (TM) in tokamaks
- First self-consistent gyrokinetic simulations of the tearing mode embedded in electromagnetic turbulence in toroidal geometry becoming available (GKW)

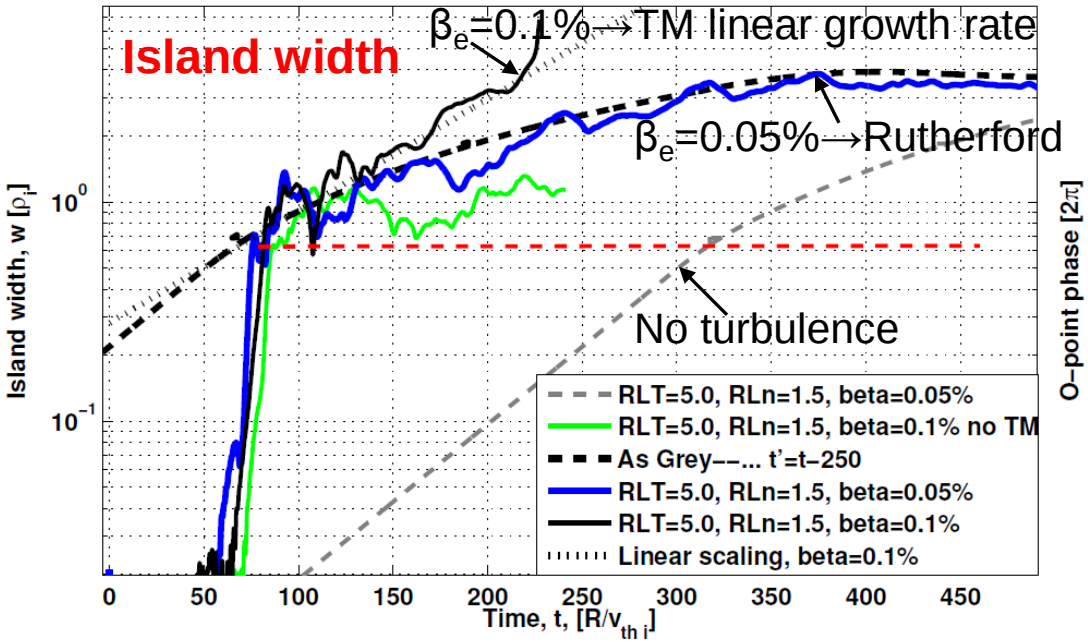

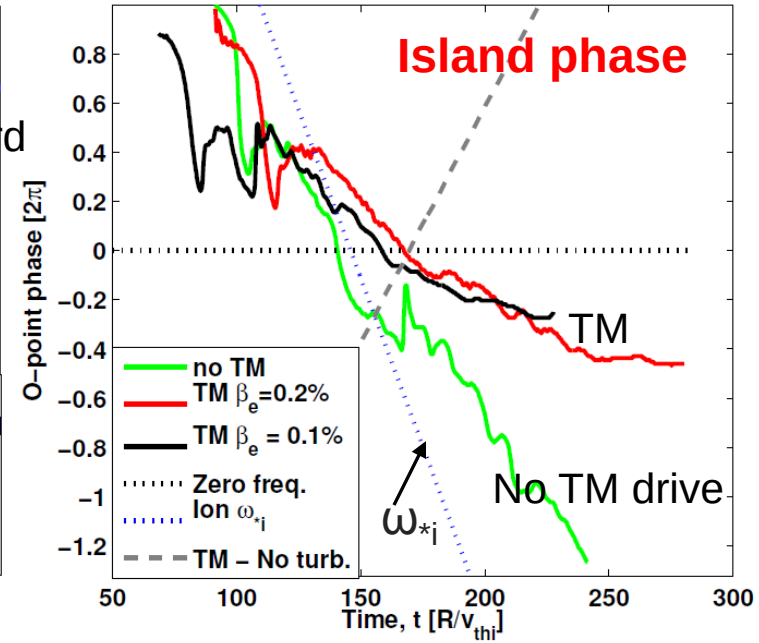

- (ITG) Turbulence seeding of magnetic islands provides fast growth of structures of the order of the ion gyroradius, further fate depends on β_e (disruption of the Rutherford phase observed, TM grows at its linear growth rate after theoretical singular layer width has been exceeded)
- Seeded islands rotate in the ion direction, slow down as they grow

Summary of completed work

- Self-consistent kinetic modeling of primary runaway formation during thermal quench (prompt conversion of the plasma current into runaway current is advantageous for plasma position control).
- Kinetic near-threshold theory for runaway sustainment and runaway avalanche in presence of synchrotron losses (enhanced critical electric field found for avalanche onset).
- Marginal stability scenario for runaway-dominated current quench (runaway avalanche threshold determines the current decay time-scale).
- Revised thresholds of runaway-driven micro-instabilities (instability window quantified for ITER-relevant parameters).

Generation of runaway electrons during the thermal quench in tokamaks

Pavel Aleynikov and Boris N. Breizman

- **Mitigated disruptions**: Maxwellian pre-quench electrons (T_0) & Impurity atoms delivered instantaneously
  - **Kinetic description** of the pre-quench electrons
  - Spitzer conductivity of the "cold" plasma (i.e. mostly impurity electrons)
  - Constant current density during TQ; the **electric field evolves** accordingly
  - "Cold" plasma temperature is determined by the power balance (i.e. line radiation)

✓ For ITER-like pre-quench profiles:

- ✓ **Prompt conversion** of full current for $n_{Ar}>10^{20}m^{-3}$
- ✓ **Negligible RE seed** current disruption for $n_{Ar}<3\times10^{19}m^{-3}$
- ✓ **Non-monotonic radial RE profile**

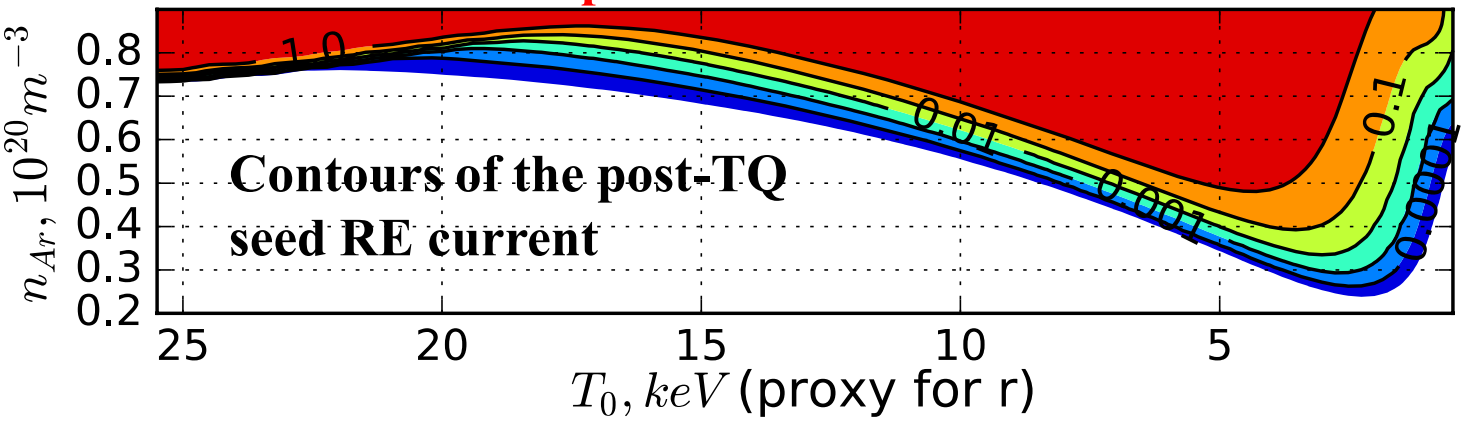

TH/P1-34
Simulation study of interaction between runaway electron generation and resistive MHD modes over avalanche timescale

A. Matsuyama, N. Aiba, and M. Yagi

National Institutes for Quantum & Radiological Science & Technology (Japan)

Highlight

- Multi-timescale simulation of runaway generation incl. seed generation during thermal quench (0.1-1ms) and avalanche growth during current quench (1-10ms) with m=1 resistive kink instability (10-100μs).
- Resistive kink can enhance primary currents through inductive electric field and radially redistributes seed currents.
- Flat seed current profile over beam radius is inherited by secondary electrons and is maintained on avalanche timescale.

→ *Our new simulation points out that resistive MHD mode in TQ phase is a possible mechanism governing current profile of runaway electrons.*

Fig. 1 Resistive kink enhance runaways with inductive electric field and yields flattening of small seed currents of 0.1-1 % of ohmic current.

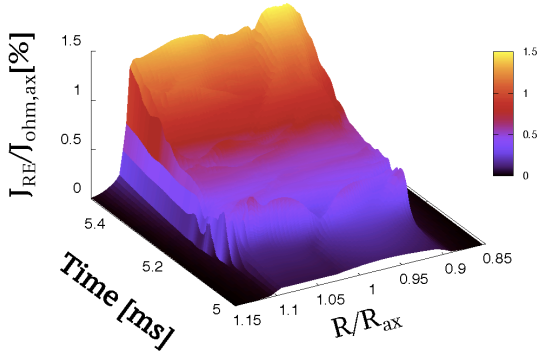

Fig. 2 Runaway current and q profile after avalanche "inherits" profile modification to small seed currents

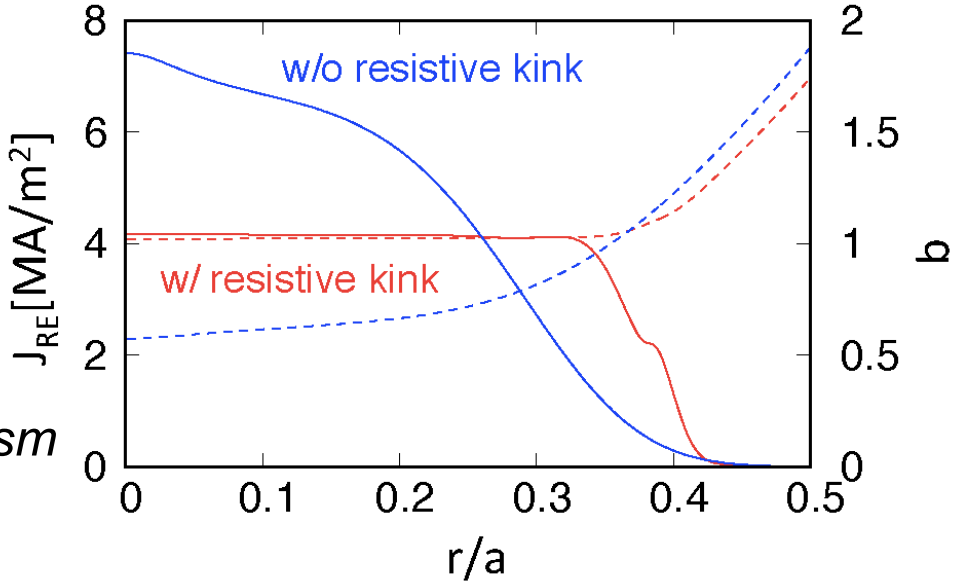

Energetic Particles

TH/P4-14 Summary: R.E. Waltz, E.M. Bass, and He Sheng
"A critical gradient model for energetic particle transport from Alfven eigenmodes: GYRO verification, DIII-D validation, and ITER projection"

- The linear rate recipe $\gamma_{AE\text{-}ITG/TEM} > \gamma_{ITG/TEM}$ for the critical gradient for Alfven eigenmode (AE) transport of energetic particles (EPs) has been verified by new local nonlinear GYRO simulations with low-n AE modes embedded in high-n ITG/TEM mode turbulence.

- The critical gradient model (CGM) has been validated by DIII-D with NBI EP's using the ALPHA EP density transport code: the importance of orbit drift broadening of the critical gradient profile in DIII-D and energy dependence of AE transport of EP's is stressed.

- The ALPHA code ITER projection for fusion alpha confinement revised with a CGM for AE simultaneous drive from (and transport of) 3.5 Mev alphas and 1Mev NBI shows that alpha AE transport losses can be doubled with the additional AE drive from the NBI.

- A more practical CGM based on the linear rates (AE threshold) determined by TGLF (and verified by GYRO linear rates) illustrates how the AE transport of NBI EPs in DIII-D gets shut-off as the current penetrates with q_{min} dropping from 4.5 to 1.0 and increasing shear: the critical gradient rising above the slowing down gradient (except at the very center).

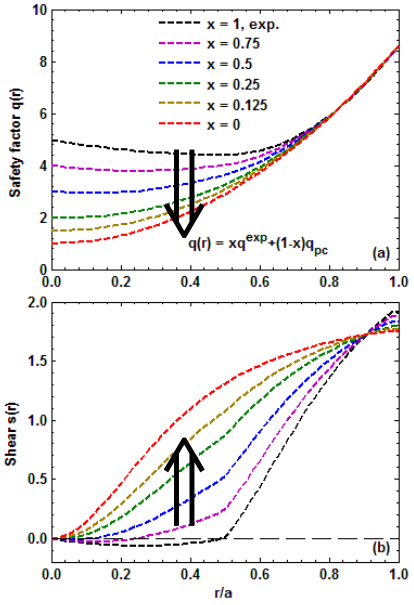

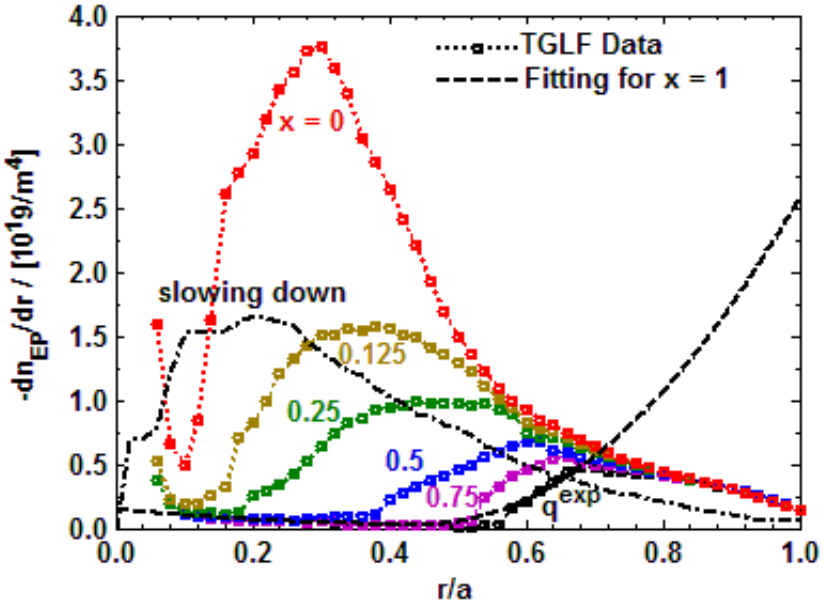

GENERAL ATOMICS

TH/4-3: First-Principle Simulations Reproduce Multiple Cycles of Abrupt Large Relaxation Events in Beam-Driven JT-60U Plasmas

A. Bierwage *et al.* (QST, Japan)

QST

IFERC-CSC

MHD-kinetic hybrid code MEGA incl. sources and collisions for beam ions has self-consistently simulated cyclic abrupt transitions from weak to strong energetic ion transport during "Abrupt Large Events (ALE)" as seen in JT-60U exp.

- Fast ion pressure lies 20-45% below classical prediction.
- Reproduced multiple ALEs with the correct period (~50ms).
- Found that fluctuations with multiple toroidal mode numbers n = 1,2,3 reach high amplitudes during ALEs.
- Sim. results were confirmed experimentally (validation).

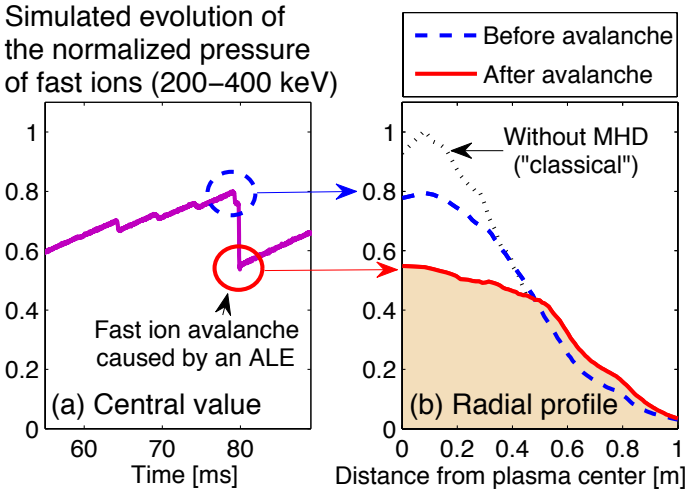

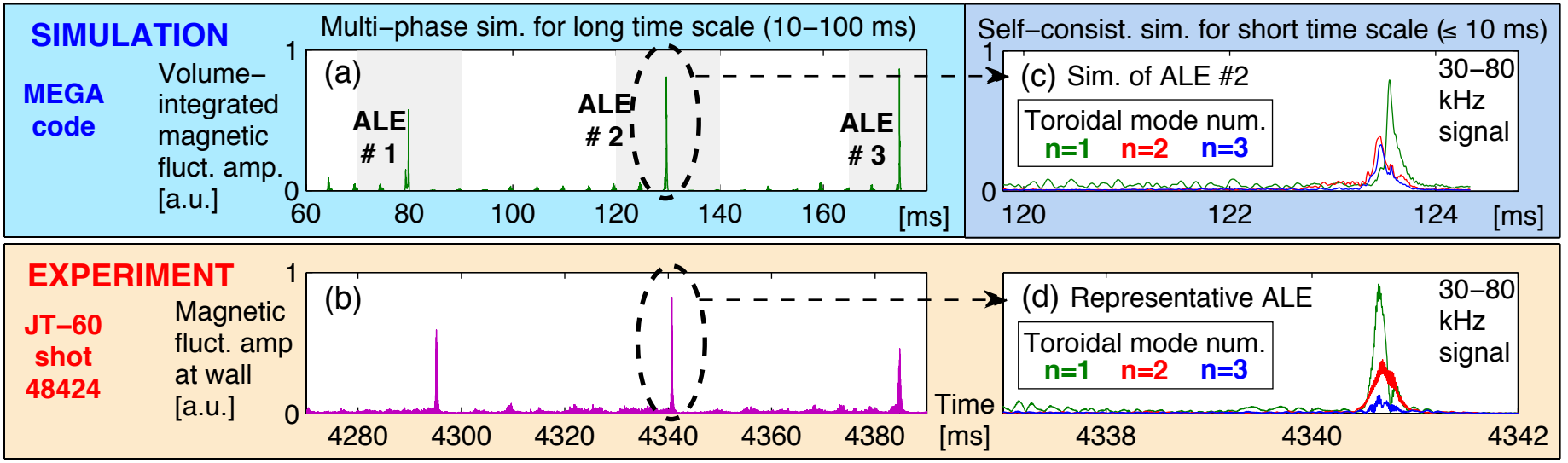

→ Major new milestone for numerical prediction and physical understanding of fast ion confinement.

Summary of Paper **PDP-10** Th (W) Ex(W)

Chirping in Plasmas; test of criterion for chirping onset & simulation of explosive chirping

by H.L. Berk, B.N. Breizman, V. Duarte, N. Gorelenkov, et. al.

1. Considers two issues: (A) How to predict whether experimental configurations with energetic particles causing Alfvenic instabilities, is likely to chirp.
(B) Numerical simulation and theory of chirping avalanche using reduced modelling equations.
2. In investigation (A), quantitative refinement of Lilley, Sharapov, and Breizman (2009)) equation used to classify likelihood for energetic particles, causing Alfvenic instability, to induce frequency chirping. Input parameters taken from TFTR, NSTX and D-III-D data.
3. Agreement between the theoretical classification and experimental data obtained only if detailed phase space dependence of physical parameters taken. For D-III-D, inclusion of diffusion of energetic particles due to background turbulence essential for agreement.
4. Demonstration of chirping suppression in D-III-D when background turbulence suppresses.
5. In investigation B, reduced theory model developed based on perturbing drift average equilibrium orbits due to excitation of Alfvenic waves.
6. Model simulates TAE and EPM instability.
7. Simulation shows time evolution of spectrum for increasing hot particle beta β_{EP} first exciting the limited chirp TAE and then the EPM with rapid long range chirping (see figure).
8. Analytic theoretical description of chirping, caused by phase space clump moving outwardly across field lines achieved. Perhaps qualitative description achieved for chirping avalanche observed in NSTX

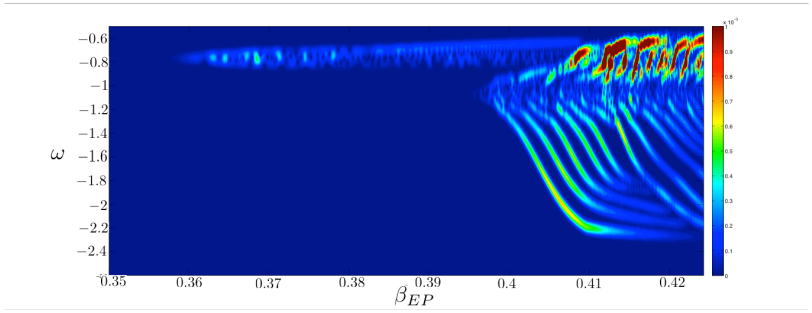

2) Turbulence scattering explains chirping NSTX Alvenic modes and steady state AMs in DIII-D

Duarte, Berk, Gorelenkov *et al*, inv talk at Sherwood'16; PRL'16 (submitted)

New NOVA criterion for frequency chirping $\sim E_{TAE} * \nu_{dr} \nu^{-4}_{drag}$

>0 (i): fixed-frequency wave likely
<0 (ii): chirping wave likely

PPPL/IFS/GA collaboration => a correlation emerged between the turbulent driven EP pitch angle scattering and frequency chirping in DIII-D

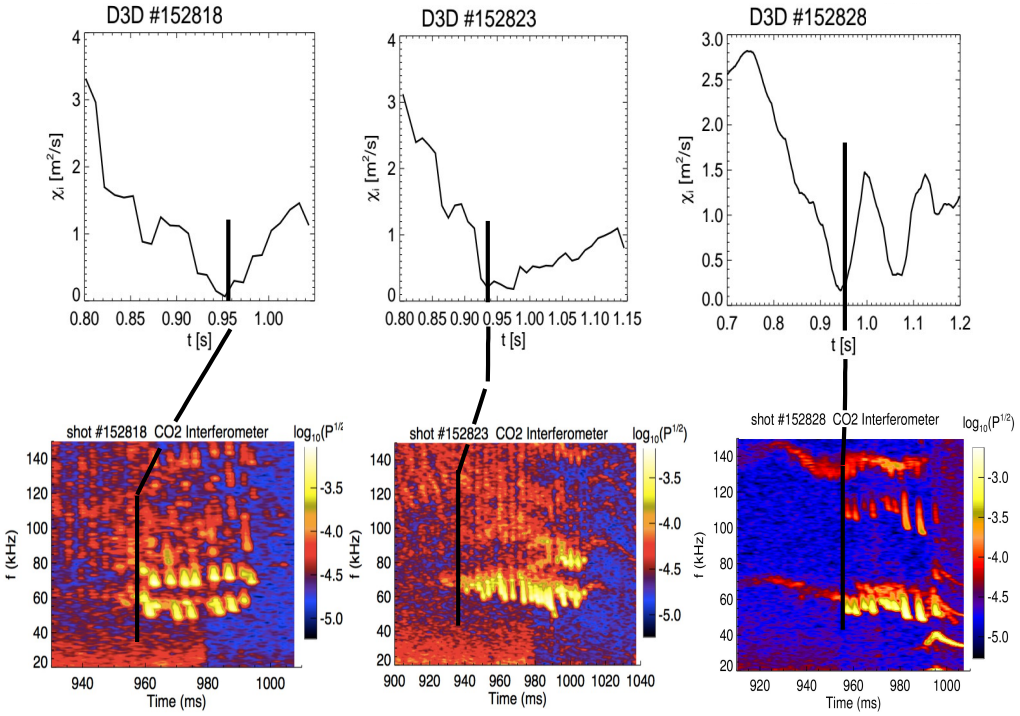

The proposed criterion is able to quantitatively explain observations

Fixed-frequencies, DIII-D and TFTR

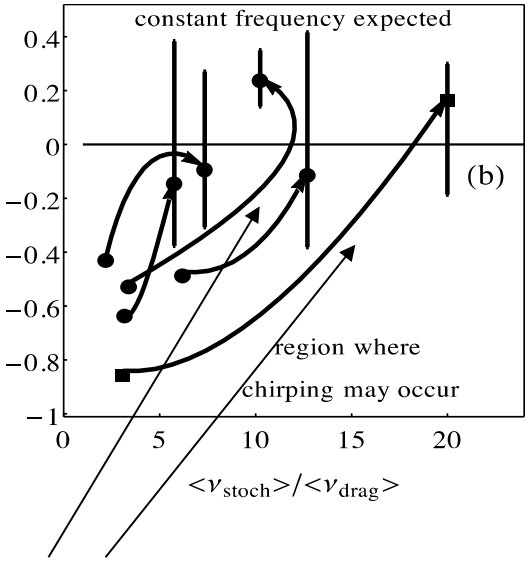

Turbulent diffusion boosts pitch-angle scattering from collisional level

Integrated Modeling

Theory-Experiment Validation Has Increased Confidence in ITER Achieving its Q=10 mission

- **Self-consistent coupling of core & pedestal theoretical models**
  - No free or fit parameters
- **Whole profile iteration converges to unique solution**
  - Predicts β_N to ~15% in 200 DIII-D cases
- **Enables prediction and optimization of ITER fusion gain: Q~12 possible**

New frontier: Multi-scale turbulence simulations and TGLF improvement

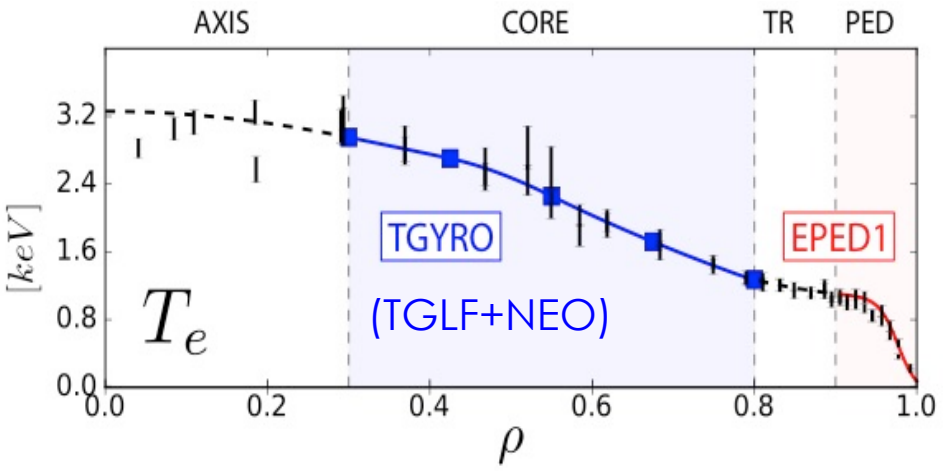

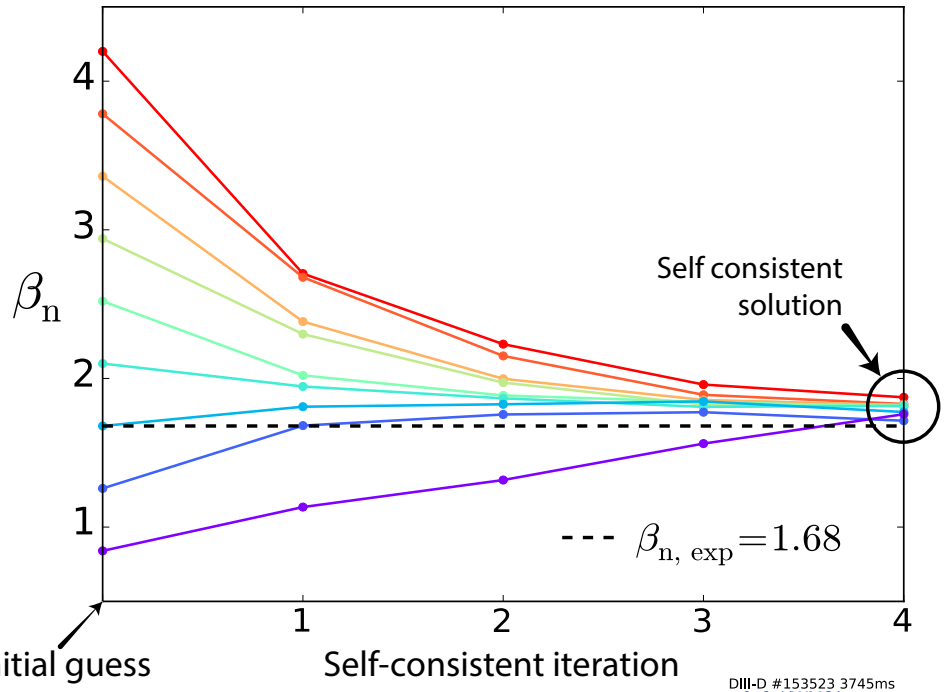

Meneghini – TH/9-1
Holland– TH/6-1
Staebler – TH/P2-8

ITER Fuelling Requirements and Scenario Development for H, He and DT through JINTRAC Integrated Modelling

E. Militello Asp, G. Corrigan, P. da Silva Aresta Belo, L. Garzotti, D.M. Harting, F. Köchl, V. Parail, M. Cavinato, A. Loarte, M. Romanelli and R. Sartori

- First ever integrated 1.5D core + 2D edge simulations of
  - He plasmas (L-mode to ELMy H-mode predicted!)
  - Current ramp-up/down scenarios
- Pellet fuelling
  - Likely to be essential for the density rise in L-mode in H, DT
  - but should preferably be moderate during the L-H transition until ELMy H-mode is reached to avoid back transition.
  - Careful tuning of pellet size/frequency needed to avoid triggering MARFEs.
- H-L transition sufficiently slow for plasma control systems to keep the plasma from touching the vessel walls.
  - Ne seeding may require real-time control to keep divertor conditions within operational range.

FUSION FOR ENERGY iter TU WIEN CCFE CULHAM CENTRE FOR FUSION ENERGY

Impressive variety of modelling done across community

- **Wide range of interpretive and predictive modelling presented from across whole fusion community**
  - See wide range of talks and posters at this conference
- Supported by community, ITER has developed a **standard data representation** to facilitate exchange of data between codes and from/to storage
  - Generic Data Model suitable for all experiments and simulations
  - Supports flexible exchange of data and software components
  - SD Pinches, TH/P2-14

Standard Data Model

- This **Data Model** is the backbone of the **ITER Integrated Modelling & Analysis Suite (IMAS)**
  - To be used for *all physics modelling activities* on ITER
    - SD Pinches, TH/P2-14
  - Based on earlier work within the EU
    - G Falchetto TH/P2-13 and I Voitsekhovitch TH/P2-12
- Adaptation of many well-known codes to IMAS (ITER Data Model) has started
  - E.g. DINA adapted to IMAS and simulations of ITER 7.5 MA scenario, respecting engineering limits, performed for a complete cycle of the poloidal field circuit (including breakdown)

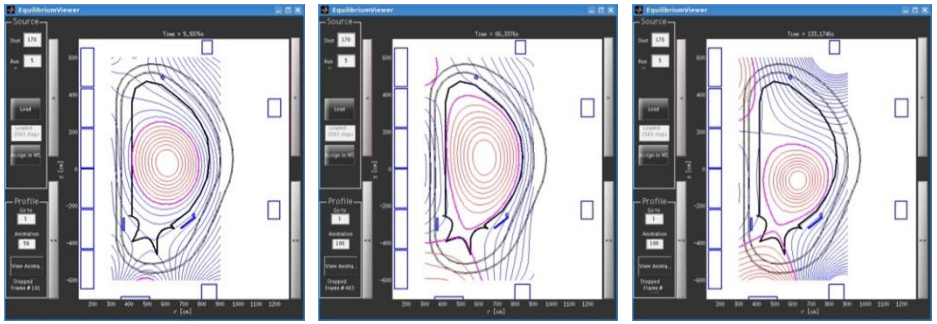

Where does fusion R&D stand right now?

- Fusion community has started developing tools and workflows in IMAS to support ITER's and their own research programmes in preparation for ITER Operation
- IMAS has started being used for ITPA activities including benchmarking, validation and data exchange
  - E.g. ITPA Energetic Particle Physics Topical Group benchmark on fast ion distributions from auxiliary heating systems for use in stability calculations

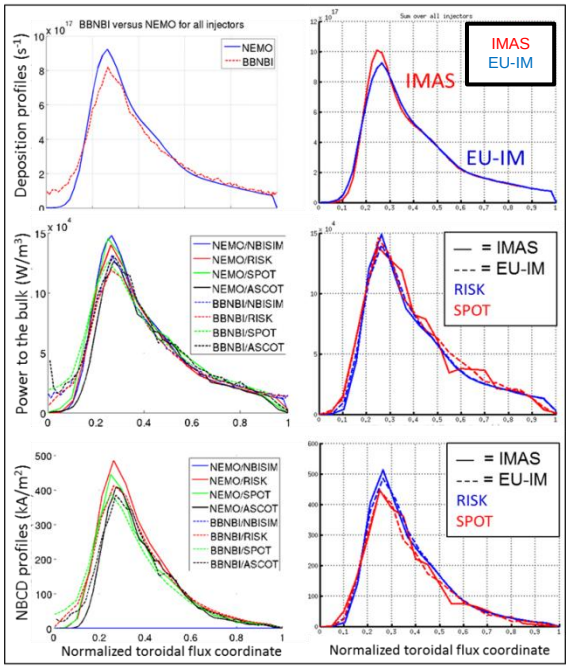

Next Steps

- Looking to future, make more progress by working together
- Use ITER modelling infrastructure (IMAS) to develop tools and workflows to support R&D programmes (including for ITER), exploiting synergies across fusion communities
- Use ITER modelling infrastructure (IMAS) within R&D facilities to validate workflows and help prepare for ITER operations
- Focus resources to simultaneously benefit both individual research programmes and ITER

Concluding remarks

“Pure theoretical” contributions ~5% O(total), BUT they do form the basis

3D physics – the round table for tokamak and stellarator studies

More than 50% of TH contributions directly address **ITER** relevant problems. **ITER** is a real drive of fusion research worldwide.

TH reports at FEC-2016 manifest

essential progress in understanding of key physics issues on the way of fusion

demonstrate **broad arsenal of advanced tools** to resolve them providing

confidence in overall success of fusion research